

AMENDMENTS TO THE DRAWINGS:

The attached replacement sheet of Figure 1 includes changes to depict the film, labeled with the number 5, as originally described in paragraph [0005] of the specification. No other substantive changes have been made to Figure 1. Because amended Figure 1 depicts an element that was previously described in the specification, this amendment does not add new matter.

Attachments: One replacement sheet for Figure 1.

REMARKS

With entry of this Amendment, claims 1-11 are pending. Applicants have amended claims 1, 3, and 10 to indicate that the pore penetrates from one end of the body to the other end. The specification supports this amendment at, for example, Figure 1 and in the Example, which describes the formation of a porous body 10 mm thick with pores up to 5 mm in depth. With pores of 5mm extending inwards from each end of the 10 mm porous body, these pores effectively extended from "one end of the body to the other end" as recited in amended claims 1, 3, and 10. Claim 4 has been amended to recite "plasma-spraying titanium powder on a plate and then being cut out." The specification supports this amendment at, for example, page 7, lines 22-28 and page 8, lines 13-18. Applicants also added new claim 11 as supported by the specification at, for example, page 2, line 28 to page 3, line 3. Applicants have also amended paragraph [0005] of the specification to indicate that the film discussed in that paragraph is now depicted on amended Figure 1 and to correct minor grammatical errors.

Neither the claim amendments nor the specification amendment introduce new matter.

Objection to the Drawings

The Office objects to the drawings because they allegedly do not show every feature of the claimed invention. Office Action, page 2. Specifically, the Office contends that the film and phases recited in claims 1 and 2 must be shown in the drawings. *Id.* Applicants attach a replacement sheet for Figure 1. This replacement sheet provides an amended Figure 1 showing the location of the film and the phase(s) that are part of the film as indicated by the number 5 in the drawing. Because the

elements of claims 1 and 2 are depicted in the drawings, Applicants request that the Office withdraw this objection.

Rejections Under 35 U.S.C. § 103

Claims 1 and 2 stand rejected under 35 U.S.C. § 103(a) as allegedly obvious over JP 5-56990 A ("Kawatani") in view of U.S. Patent 5,609,633 ("Kokubo"). Office Action, page 3. According to the Office, Kawatani teaches a "porous body comprising a lump of titanium or titanium alloy . . . and having a porosity of 40-60% . . . , the body having a pore interconnected in a three-dimensional network with a diameter of 100 to 3000 μm and a hole/ extremely minute pores with a diameter of 50 μm or less on an inner surface of the pore." *Id.* Considering the varied diameters of the pores in Kawatani, the Office reasons, it is "inevitable" that the claimed structure of a hole on an inner surface of the interconnected pore would appear. *Id.* The Office acknowledges that Kawatani does not teach a film comprising at least one phase selected from the group consisting of an amorphous titanium oxide phase, an amorphous alkali titanate phase, an anatase phase and a rutile phase aligned with (101) plane. *Id.*

The Office contends that Kokubo teaches a film comprising at least one phase selected from the group consisting of an amorphous titanium oxide phase, an amorphous alkali titanate phase, an anatase phase and a rutile phase aligned with (101) plane at column 2, lines 4-13. *Id.* at 4. The Office admits that Kokubo does not teach all of the claimed effects and physical properties, but because this reference allegedly teaches all of the claimed ingredients, process steps, and process conditions, the claimed effects and properties would be "implicitly" achieved. *Id.* Kokubo also allegedly teaches that the desirable thickness of the film is 0.1 to 10 μm . *Id.*

Taking each of these alleged teachings, the Office concludes that it would have been obvious to combine the film/layer allegedly taught by Kokubo with the porous endosseous implant of Kawatani. *Id.* at 4. According to the Office, one would have been motivated to do so because Kokubo suggests that a substrate covered by a film including a phase of alkali titanate would induce the growth of apatite and thus increase the ability of the implant to bond with bones of the body. *Id.*

Applicants traverse because neither Kawatani nor Kokubo alone or in combination teach the structure described in independent claim 1. As Applicants will explain, the Office confuses the "rough film" of Kawatani with the "porous body" of claim 1. To clarify this distinction, Applicants amended claim 1 to indicate that the pore penetrates from one end of the porous body to the other end.

The invention in Kawatani focuses on generating a "rough film" with "high porosity" on the *surface* of a "base material." See paragraph [0005] at page 3 of the English translation. Indeed, Kawatani generates these rough films in two ways: (1) the rough film is formed on the base material by plasma spraying and (2) the rough film is formed by alternating plasma sprays using coarse particles with plasma sprays using fine particles so that the fine particles act as a bonding layer between the coarse particles (see attached referential Figure 3). Consistently, Kawatani focuses on forming this "rough film" on the surface of the base material. See paragraph [0009] ". . . are bound to one another and also, under this condition, bound to the surface of the base material layer."; paragraph [0013] ". . . thereby forming a rough film having a pore size of 150 to 350 μm on the surface of the base material."

In contrast, the invention of claim 1 has a porous body "comprising a lump of titanium or titanium alloy and having a porosity of 30 to 80%, the body having a pore interconnected in a three-dimensional network with a diameter of 100 to 3000 μm and a hole with a diameter of 50 μm or less on an inner surface of the pore, the pore penetrating from one end of the body to the other end." In Kawatani, the rough film sits on the surface of a base material. Any "pores" that may be present in this rough film clearly do not extend through the base material to the other side because this rough film merely sits on its surface. To assist the Office in recognizing the distinction between the structure of Kawatani's implant and the artificial bone of the invention, Applicants discuss one of the ways in which the porous body of the invention can be made.

In one method, a macro-porous titanium layer is formed on a plate by plasma spraying titanium powder, as diagrammed on attached referential Figures 1 and 2. The "porous body" of claim 1 is formed by cutting the resulting porous layer from the plate. See step 3 in referential Figure 1. The in this porous body, the pore penetrates from one end of the porous body to the other end, conferring osteoinductivity to the artificial bone. Unlike the instant invention, the "pores" in the rough film of Kawatani do not extend across the thickness of the base material and instead one end of the pore is closed off by the base material itself as shown in attached referential Figure 4.

Applicants also note that Kawatani's implant requires the presence of a base material to which the rough film is attached to facilitate attachment of the base material to the body via the rough film in a process called "bioactivity." See Kawatani at paragraph [0021]. In contrast, the claimed artificial bone has "osteoinductivity," which is the ability to facilitate bone formation even in a body location where bone does not

normally form. And, *arguendo*, even if one could form the film recited in claim 1 on the "rough film" of Kawatani, which would be difficult to achieve, the coated "rough film" would not be osteoinductive as recited in claim 1 because bone formation via osteoinduction begins not at the periphery of an implant, but at the center of the implant. See attached Takemoto et al., *Biomaterials* 27:2682-91 (2006), section 3.2.2. Thus, Kawatani does not teach the "porous body" recited in claim 1.

Combining Kawatani with Kokubo does not remedy these defects in Kawatani because Kokubo teaches only the bioactivity of apatite formed on a titanium plate to enhance bonding of bone to the plate. Kokubo does not discuss osteoinductivity nor does Kokubo teach a "porous body" in which the pore penetrates from one end of the porous body to the other end, conferring osteoinductivity to the artificial bone. The Office has acknowledged this in its double patenting rejections as discussed below.

Finally, the Office has suggested that it is "inevitable" that the claimed structure of a hole on an inner surface of the interconnected pore would appear in Kawatani's rough film. Applicants request that the Office explain why it believes that the "pore interconnected in a three-dimensional network with a diameter of 100 to 3000 μm and a hole with a diameter of 50 μm or less on an inner surface of the pore" would "inevitably" be present in Kawatani and provide evidence to support its theory. Applicants note that the Office has used this rationale to support several of the rejections in this Office Action. See, e.g., Office Action at pages 8, 10, 11, 13, and 14.

In sum, the combination of Kawatani with Kokubo does not teach the "porous body" recited in independent claim 1. Because this element is absent in both

references, their combination cannot render claims 1, 2, and new claim 11 obvious. Applicants therefore request that this rejection be withdrawn.

The Office rejects claims 3-9 under 35 U.S.C. § 103(a) as allegedly obvious over Kawatani in view of Kokubo. Office Action, page 5. According to the Office, Kawatani teaches a method of manufacturing an artificial bone implant comprising providing a porous body having a porosity of 40-60%, the body having a pore interconnected in a three-dimensional network with a diameter of 100 to 3000 μm and a hole/ extremely minute pores with a diameter of 50 μm or less on an inner surface of the pore. *Id.* Considering the varied diameters of the pores in Kawatani, the Office reasons, it is "inevitable" that the claimed structure of a hole on an inner surface of the interconnected pore would appear. *Id.* As the Office acknowledges, however, Kawatani does not teach immersing the artificial bone implant in an alkaline aqueous solution, but contends that Kokubo teaches this at column 2, lines 29-32. According to the Office, it would have been obvious to combine Kokubo's method of manufacturing an artificial bone with the "porous body" implant allegedly taught in Kawatani. *Id.* One of ordinary skill in the art would allegedly have been motivated to do so because the method of Kokubo creates an outer surface rich in alkali ions that eventually forms a titanium hydroxide phase which readily reacts with calcium and phosphorous. Applicants traverse.

As discussed above, the Office's interpretation of Kawatani is flawed. This reference does not teach a "porous body" as the Office suggests. Rather, it teaches a "rough film" that sits on a "base material." Thus, Kawatani does not teach the step of "providing a porous body" as recited in claim 3. Kokubo does not teach this porous

body either. Thus, the combination of Kawatani and Kokubo cannot teach a method of manufacturing an artificial bone as recited in independent claim 3.

Regarding claims 4-6, the Office alleges that Kawatani teaches plasma-spraying titanium powder on a sprayed body and considers the bottom layers of the plasma spray to be a "sprayed body." Office Action, page 6. Applicants note that claim 4 has been amended to recite "wherein the body is obtained by plasma-spraying titanium powder on a plate and then being cut out." Neither Kawatani nor Kokubo teach such a step, where the porous body is formed by being cut from the plate. Thus, the combination of these references cannot render claims 4-6 obvious.

Regarding claims 7 and 8, the Office acknowledges that Kawatani does not teach immersing the porous body in an alkaline aqueous solution, but suggests that Kokubo teaches this followed by heating the artificial bone substitute. *Id.* Specifically, Kokubo allegedly teaches that a desirable heating temperature is 300 to 800 °C. *Id.* at 7. One of ordinary skill in the art would allegedly have been motivated to immerse the porous body in an alkaline aqueous solution and then to heat it because doing so causes the diffusion of oxygen, increases the thickness of the formed film/phase, and allows apatite to form on the film/surface layer. *Id.* at 6 and 7. As Applicants have explained, the combination of Kawatani and Kokubo does not render the method of independent claim 3 obvious and therefore cannot render dependent claims 7 and 8 obvious.

Regarding claim 9, the Office acknowledges that Kawatani does not teach immersing the body in water after immersing in an alkaline aqueous solution, but relies on Kubuko for this teaching, citing column 4, lines 18-23. According to the Office, one would have been motivated to carry out this additional step to clean the porous body to

make it useful as a bone substitute. Office Action, page 7. The combination of Kawatani and Kokubo does not render the method of independent claim 3 obvious and therefore cannot render dependent claim 9 obvious. Neither reference teaches the step of “providing a porous body” as recited in claim 3.

Because the combination of Kawatani and Kokubo does not render claims 3-9 obvious, Applicants request that this rejection be withdrawn.

Claim 10 stands rejected under 35 U.S.C. § 103(a) as allegedly obvious over Kawatani in view of U.S. Patent 6,689,170 (“Larsson”). Office Action, page 8. The Office applies Kawatani as discussed above and notes that Kawatani does not teach anodizing the porous body in an electrolytic solution. *Id.* The Office turns to Larsson for the alleged teaching of an implant for permanent anchorage in bone tissue which is made of titanium with a titanium oxide surface that has been modified by anodization. The Office concludes that it would have been obvious to combine the method of anodizing in Larsson with the “porous body” taught in Kawatani because anodization increases the oxide thickness on the titanium surface and titanium oxide is suspected to increase the biocompatibility of titanium. *Id.* at 8 and 9. Applicants traverse.

As Applicants noted above, Kawatani does not teach a “porous body” as described in claim 10 and therefore does not teach the step of “providing a porous body” as recited in this claim. Like Kawatani, Larsson focuses on making modifications to the surface of a base material. In the case of Larsson, the base material is a titanium disc made from a titanium rod. See col. 11, lines 49-53. The implants were treated three ways: machined, electropolished, and electropolished with anodization. See col. 11, lines 54-58. While Larsson explained that anodization caused some roughness on

the surface of the implant, it was relatively smooth compared to surfaces treated with plasma spraying. See col. 20, lines 36-50. Thus, Larsson's anodization of the titanium implant did not give rise to "a pore interconnected in a three-dimensional network with a diameter of 100 to 3000 μm and a hole with a diameter of 50 μm or less on an inner surface of the pore." Even if it did, the pore could not penetrate "from one end of the body to the other end" as recited in claim 10 because the "pores" would only be formed on the surface of the titanium disc. Thus, because the combination of Kawatani and Larsson do not teach the step of "providing a porous body" as recited in claim 10, these references do not render claim 10 obvious. Accordingly, Applicants request that the Office withdraw this rejection.

Rejections Based on Obviousness-Type Double Patenting

The Office rejects claim 1 based on the judicially created doctrine of obviousness-type double patenting in light of claim 1 of Kokubo. Office Action, page 9. According to the Office, claim 1 of Kokubo recites an artificial bone repairing material with a primary surface layer comprising at least one phase selected from the group consisting of an amorphous titanium oxide phase, an amorphous alkali titanate phase, an anatase phase and a rutile phase aligned with (101) plane. *Id.* The Office admits that Kokubo does not teach all of the claimed effects and physical properties, but because this reference allegedly teaches all of the claimed ingredients, process steps, and process conditions, the claimed effects and properties would be "implicitly" achieved. *Id.* at 10. The Office also acknowledges that claim 1 of Kokubo does not teach the porous body and the dimensions of the holes a pores and turns to Kawatani for the alleged teaching of a porous body. *Id.* Applicants traverse.

As Applicants have discussed above, Kawatani does not teach the recited porous body of pending claim 1. The Office admits that claim 1 of Kokubo also does not teach this porous body. Thus, the combination of claim 1 of Kokubo and Kawatani does not provide any guidance on the use of the recited porous body as an osteoinductive artificial bone or on how to manufacture such a porous body. Instant claim 1 is therefore not an obvious variant of Kokubo's claim 1. Applicants request that this rejection be withdrawn.

The Office has also posed additional obviousness-type double patenting rejections using the same general logic of relying on a claim from Kokubo and matching that claim with Kawatani's alleged teaching of a porous body. For example, the Office rejected pending claim 2 in light of Kokubo's claim 3 and Kawatani and rejected pending claims 3-7 in light of Kokubo's claim 8 and Kawatani. Office Action, pages 11-17. In each of these rejections, the Office again admits that the claims of Kokubo do not teach the porous body recited in the instant claims and relies on Kawatani for this teaching. See, e.g., Office Action, page 11. Applicants contend that these rejections must fall for the same reason indicated above for pending claim 1. Kawatani does not teach the porous body recited in independent claims 1 and 3 and thus does not compensate for the deficiency of the claims in Kokubo as acknowledged by the Office. Accordingly, claims 2 and 3-7 are not obvious variants of claims 3 and 8 in Kokubo, respectively. Applicants request that this rejection be withdrawn.

Conclusions


In view of the foregoing amendments and remarks, Applicants respectfully request reconsideration and reexamination of this application and the timely allowance of pending claims 1-11.

Please grant any extensions of time required to enter this response and charge any additional required fees to Deposit Account 06-0916.

Respectfully submitted,

FINNEGAN, HENDERSON, FARABOW,
GARRETT & DUNNER, L.L.P.

Dated: November 29, 2007

By: 
Maryann T. Puglielli
Reg. No. 52,138

Attachments: A replacement sheet for Figure 1, referential Figures 1-4, and Takemoto et al., *Biomaterials* 27:2682-91 (2006).



Osteoinductive porous titanium implants: Effect of sodium removal by dilute HCl treatment

Mitsuru Takemoto^{a,*}, Shunsuke Fujibayashi^a, Masashi Neo^a, Jun Suzuki^b,
Tomiharu Matsushita^b, Tadashi Kokubo^c, Takashi Nakamura^a

^aDepartment of Orthopaedic Surgery, Graduate School of Medicine, Kyoto University, Shogoin, Kawahara-cho 54, Sakyo-ku, Kyoto 606-8507, Japan

^bKobe Steel, Ltd., Kobe, 1-5-3 Takatsukadai, Nishi-ku, Kobe 651-2271, Japan

^cResearch Institute for Science and Technology, Chubu University, 1200 Matsumoto-cho, Kasugai 487-8501, Japan

Received 29 June 2005; accepted 29 December 2005

Abstract

In a previous study, we observed that chemically and thermally treated plasma-sprayed porous titanium possesses intrinsic osteoinductivity and that bone formation occurs after 12 months in the muscles of beagle dogs. The aim of this study was to optimize the surface treatment and to accelerate the osteoinductivity. Previous studies have reported that sodium removal converts the sodium titanate layer on the surface of an alkali-treated titanium plate into a more bioactive titania layer. In this study, we developed a dilute hydrochloric acid (HCl) treatment for porous titanium, which removed sodium from the complexly shaped porous structure more effectively than conventional hot water treatment. Three types of surface treatments were applied: (a) alkali and heat treatment (AH treatment); (b) alkali, hot water, and heat treatment (Water–AH treatment); and (c) alkali, dilute HCl, hot water, and heat treatment (HCl–AH treatment). The osteoinductivity of the materials implanted in the back muscles of adult beagle dogs was examined at 3, 6, and 12 months. The HCl–AH-treated porous bioactive titanium implant had the highest osteoinductivity, with induction of a large amount of bone formation within 3 months. The dilute HCl treatment was considered to give both chemical (titania formation and sodium removal) and topographic (etching) effects on the titanium surface, although we cannot determine which is the predominant factor. Nevertheless, adding the dilute HCl treatment to the conventional chemical and thermal treatments is a promising candidate for advanced surface treatment of porous titanium implants.

© 2006 Elsevier Ltd. All rights reserved.

Keywords: Osteoinduction; Osteogenesis; Titanium; Porous; Metal surface treatment; Titanium oxide

1. Introduction

The term “bioactivity” is defined as tissue-bonding ability [1]. Bioactive materials include bioglass, hydroxyapatite (HA), other calcium phosphate-based biomaterials, and glass-ceramic A–W, which can bond to living bone directly [1]. When these bioactive materials have a porous structure, they sometimes become osteoinductive in soft tissues without the addition of osteogenic cells or bone morphogenetic protein [2–9].

We recently showed that even titanium metal containing no calcium phosphate could be osteoinductive when it has

complex interconnecting porous structures and a bioactive surface activated through specific chemical and thermal treatments [10]. However, the implantation period required for bone induction in this porous bioactive titanium was longer (12 months) than in previously reported porous CaP-based biomaterials (45–90 days). In an early report of osteoinduction by a polymeric sponge in the pig, Winter and Simpson commented [11] that *in vivo* calcification (or “apatite formation”) is believed to be the precursor of bone induction in CaP-free biomaterials [10,12–14], which may provide one reason for the delayed osteoinduction by the porous bioactive titanium implants [13].

Before the development of porous bioactive titanium, titanium plates were used to develop the chemical and thermal treatments that convert titanium and titanium alloys into

*Corresponding author. Tel.: +81 75 751 3365; fax: +81 75 751 8409.
E-mail address: m.take@kuhp.kyoto-u.ac.jp (M. Takemoto).

bioactive materials [15–22]. Alkali and heat treatment was the earlier bioactive treatment for titanium metal, and it produced a bioactive sodium titanate layer on the surface of titanium metal [15–17,19,20,22]. Subsequent studies revealed that sodium removal by hot water immersion enhanced the bioactivity of alkali- and heat-treated titanium plates [18,21]. Titania with specific structures (e.g., anatase) on the sodium-free bioactive titanium is more bioactive than sodium titanate. Therefore, in developing bioactive treatments for porous titanium, we also applied sodium removal by water treatment between alkali and heat treatments [10]. However, unlike titanium plate with a simple two-dimensional structure, it was not easy to remove sodium from porous titanium by conventional hot water treatment because of its complex three-dimensional porous structure: water-treated conventional porous bioactive titanium implants retained sodium and the sodium titanate layer with limited formation of titania layers.

To overcome these problems, in addition to water treatment, we have developed a dilute hydrochloric acid (HCl) treatment for porous titanium implants, which almost completely removes sodium, even from deep pores. We hypothesized that this dilute HCl-treated porous titanium would possess improved bioactivity and osteoinductivity accompanying the formation of the titania layers. The aim of this study was to investigate the effect of sodium removal by dilute HCl treatment on the osteoinductivity of porous bioactive titanium implants. The osteoinductivity was evaluated by implantation into the back muscles of adult beagle dogs.

2. Materials and Methods

2.1. Materials

Porous plasma-sprayed titanium blocks (porosity, 41%; pore size, 300–500 µm; yield compression strength, 85.2 MPa) were manufactured using methods described previously [23]. Briefly, a macroporous titanium layer was formed on a titanium substrate by plasma spraying with commercial pure titanium powder consisting of a mixture of a 20% volume fraction of small particles of around 50 µm in size and an 80% volume fraction of large particles of around 300 µm. Cylinders 6 mm in diameter and 15 mm in length were cut from the porous layer using an electric discharge. The titanium implants were subjected to three types of surface treatment: alkali and heat treatment (AH), water-treated AH treatment (Water-AH), and dilute HCl-treated AH treatment (HCl-AH). For the AH group, the titanium substrates were immersed in 5 ml of aqueous 5M NaOH solution at 60 °C for 24 h (alkali treatment), washed gently with distilled water, and dried at room temperature for 24 h. The implants were then heated to 600 °C at a rate of 5 °C/min, kept at 600 °C for 1 h, and then allowed to cool in the furnace (heat treatment). For the Water-AH group, the implants were immersed in ultrapure water at 40 °C for 48 h between the alkali and heat treatments. For the HCl-AH group, the implants were immersed in 0.5M HCl (pH, 3.4) at 40 °C for 24 h followed by water treatment for 24 h between the alkali and heat treatments. The porous titanium implants were supplied by Kobe Steel Ltd., Kobe, Japan.

2.2. Characterization of the surface treatment

To observe the inner pores, porous bioactive titanium was fractured using pliers. The effect of the surface treatment was analyzed using

scanning electron microscopy (SEM; S-4700, Hitachi Ltd., Tokyo, Japan), an energy dispersive X-ray microanalyzer connected to the SEM (SEM-EDX: EMAX-7000, Horiba Ltd., Kyoto, Japan), thin-film X-ray diffractometry (TF-XRD: RINT-1500, Rigaku Co., Tokyo, Japan), a mercury intrusion porosimeter (AutoPore IV 9500, Shimadzu Co., Ltd., Kyoto, Japan), and a nitrogen gas adsorption study (TriStar 3000, Shimadzu Co., Ltd., Kyoto, Japan).

The SEM-EDX quantification was determined using the standardless ZAF method, and recalculated to 100% for the two elements of Na and Ti. We used an acceleration voltage of 15 kV, a working distance of 12 mm, and an EDX collection time of 60 s. The recording of the spectra was controlled by a software package provided by the manufacturer of the EDX unit, and the measurements were carried out manually at 3000× magnification. Five to six randomly selected points in the central area (2.5–3.0 mm from the periphery) of each sample were analyzed. The penetration depth of focused electrons into the sample was calculated to be about 1.5 µm.

The TF-XRD measurements were performed using a Cu-Kα X-ray source at 40 kV and 200 mA, and a glancing angle of 1 against the incident beam. Under these conditions, the calculated detectable depth of the surface layer is around 0.2 µm, although because of complex macro- and microporous structure, we should not interpret our TF-XRD data quantitatively.

Using a mercury intrusion porosimeter, the pore size distribution of each implant was expressed using the logarithmic differential intrusion volume as a function of pore diameter. For the measurements of surface topography, micropores with a diameter lower than 10 µm were mainly analyzed. From the results of the nitrogen gas adsorption study, the specific surface area was calculated by the BET method.

The apatite-forming ability of the samples was examined by soaking them in simulated body fluid (SBF), which had a pH of 7.40 and ion concentrations of Na⁺, 142.0 mmol/l; K⁺, 5.0 mmol/l; Ca²⁺, 2.5 mmol/l; Mg²⁺, 1.5 mmol/l; Cl⁻, 147.8 mmol/l; HCO₃⁻, 4.2 mmol/l; HPO₄²⁻, 1.0 mmol/l; and SO₄²⁻, 0.5 mmol/l [24,25]. To evaluate the apatite-forming ability of the peripheral and central areas of the pores in the interior simultaneously, fractured samples were soaked in 30 ml of the SBF for 1, 3, or 7 days at 36.5 °C, then removed from the SBF, washed with distilled water, and dried on a clean bench. The surface of the samples was examined by SEM, and any apatite formed was identified when island-like spherulites were observed, consisting of tiny flake-like crystals, which are the characteristic morphology of apatite deposited from SBF [15,17,18,24–27].

2.3. Animal experiments

This animal study was approved by the Animal Research Committee, Graduate School of Medicine, Kyoto University, Japan. Three types of implants were implanted in the dorsal muscles of 11 mature beagle dogs (weight, 10–11 kg), for periods of 3, 6, or 12 months. The animals were anesthetized by intramuscular administration of ketamine hydrochloride (50 mg/kg), followed by diazepam (5 mg) and atropine sulfate (0.5 mg) without endotracheal intubation. Just before the operation, a dose of 10 mg/kg of pentobarbital sodium was injected intravenously. During the operation, the dogs received an intravenous infusion of saline containing isoprenaline sulfate antibiotic. The operations were performed under standard sterile conditions. After incising the skin and fascia, muscle pouches were carefully made in the dorsal muscle to limit any bleeding. One of each of the above-mentioned implants (AH, Water-AH, HCl-AH) was implanted separately in each pouch, maintaining enough distance (more than 15 cm) between each sample to prevent intersample contact (three implants per animal). Each pouch was marked with 3–0 nylon to facilitate explantation. Animals were killed at 3 months (four animals, 12 implants), 6 months (four animals, 12 implants), and 12 months (three animals, nine implants) after implantation using an overdose of intravenous pentobarbital sodium.

2.4. Histological examination

Following explantation, the implant sites were removed and prepared for histology. The specimens were fractured using pliers and divided into

two equal parts. The parts of the specimens were fixed in 10% phosphate-buffered formalin, pH 7.25, for 7 days and dehydrated in serial concentrations of ethanol (70%, 80%, 90%, 99%, 100%, and 100% v/v) for 3 days at each concentration, and embedded in polyester resin. Thick sections (250 μm) were cut with a band saw (BS-3000CP, EXACT cutting system, Norderstedt, Germany) perpendicular to the axis of the implant, and ground to a thickness of 40–50 μm using a grinding-sliding machine (Microgrinding MG-4000, EXACT). Each section was then stained with Steven's blue and Van Gieson's picrofuchsin. A thorough microscopic analysis was performed on histological slides using transmitted light microscopy (Nikon Model Eclipse 80i, Nikon, Tokyo, Japan) combined with a digital camera (Nikon Model DS-5M-L1, Nikon). The other half of the specimen was prepared for surface analysis of the inner pore of the implants after implantation by washing in sodium hypochlorite solution to remove the soft tissue, fixation in 10% phosphate-buffered formalin for 3 days, and dehydration in serial concentrations of ethanol (70%, 80%, 90%, 99%, 100%, and 100% v/v) for 1 day each. Specimens were soaked in isopentyl acetate solution for 1 day and dried in a critical-point drying apparatus (HCP-2, Hitachi Ltd., Tokyo, Japan), then coated with carbon and the fracture surface examined by SEM and SEM-EDX.

2.5. Histomorphometric examination

An automated sequential-tiling approach was used to constitute a multiple-field image (2×2 mosaic) of the histological section using a software tool (PanoramaMakerTM3, Aresoft Inc., Fremont, CA, USA). New bone rate (%) was measured on a personal computer using Adobe Photoshop 7.0 (Adobe Systems Inc., San Jose, CA, USA) and ImageJ (National Institutes of Health, Bethesda, MA, USA), which was defined as the fraction of bone area in the porous area available for new bone growth.

2.6. Statistical analysis

All data are expressed as mean \pm standard deviation (SD) and were analyzed using JMP IN 5.1 (SAS Institute, Cary, NC, USA). The data were analyzed by one-way analysis of variance (ANOVA) followed by

Tukey–Kramer multiple-comparison post hoc tests to compare the implant types (AH, Water–AH, and HCl–AH) at each time point (3, 6, and 12 months postimplantation). $P < 0.05$ was considered significant.

3. Results

3.1. In vitro evaluation

3.1.1. Surface characteristics before implantation

SEM examination of the inner pores revealed that each implant possessed a microporous structure that covered the deep pores of the implants (Figs. 1A–C). The microporous structure of the HCl–AH implants was more complex than the others, and it showed a combination of large and small microporous structures (Fig. 1C). Fig. 2 shows pore size distribution curves as measured by mercury-intrusion porosimetry. The macropore distribution was almost equal among implants (Fig. 2A). The micropore distribution (pore diameter lower than 1.0 μm) of the HCl–AH implants was bimodal with a small broad peak below 0.1 μm and a larger definitive peak at around 0.5 μm , while those of other implants was unimodal with one definitive peak mainly situated around 0.1 μm (Fig. 2B). These results were consistent with the observations from the SEM micrographs and indicate the complexity of the surface of the HCl–AH implants. From the nitrogen gas adsorption study, the specific surface areas were 0.2711 m^2/g for the AH implants, 0.2946 m^2/g for the Water–AH implants, and 0.3250 m^2/g for the HCl–AH implants.

SEM-EDX analysis of the central area detected no apparent Na peak on the surface of the HCl–AH implants. The surface Na ratio ($\text{Na}/(\text{Na} + \text{Ti})$, weight percent) for

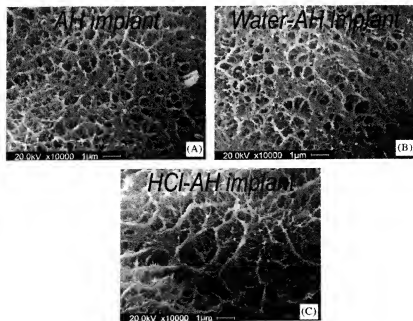


Fig. 1. Surface characteristics of the inner pores of each implant. (A) AH implant, (B) Water–AH implant, (C) HCl–AH implant. The microporous surface structure of each implant is apparent in the SEM images. Note the specific surface structure of the HCl–AH implant, with a combination of large and small micropores.

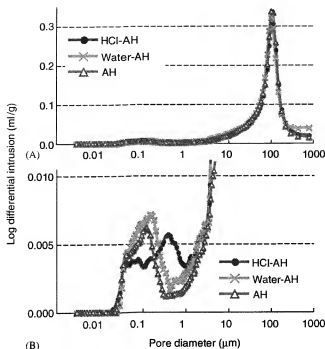


Fig. 2. Logarithmic differential intrusion as a function of pore diameter by mercury intrusion porosimetry. (A) Macropore distributions are almost equal between each implant. (B) To analyze micropores with diameter lower than 10 μm , the scale of the y-axis is enlarged. Note the bimodal distribution for the HCl-AH implant (broad one below 0.1 μm , the other between 0.1 and 1 μm), compared with the unimodal distributions for the AH and the Water-AH implants (around 0.1 μm).

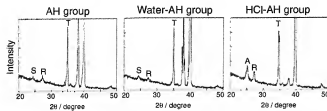


Fig. 3. XRD patterns confirmed the formation of titania with anatase and rutile structures in the HCl-AH implant. T, titanium; S, sodium titanate; R, rutile; A, anatase.

each sample was 11.5% (SD 2.1%) for the AH group, 5.7% (2.3) for the Water-AH group, and 0.0% (0.0) for the HCl-AH group. Fig. 3 shows the XRD patterns of each implant. The AH and Water-AH groups showed small XRD peaks that were ascribed to sodium titanate and rutile structures. In contrast, an anatase peak and larger rutile peak were observed in the HCl-AH group. These results indicate that, in the HCl-AH implants, sodium was effectively removed from the alkali-treated porous titanium, which was subsequently converted into titania with anatase and rutile structures after heat treatment.

3.1.2. Assessment of *in vitro* apatite-forming ability

Fig. 4 shows SEM photographs of the surfaces of each implant after immersion in the SBF. The apatite-forming

ability was high in all groups, and island-like spherulites representing apatite deposits could be recognized on the surface of all implants within 1 day of soaking in the fractured titanium blocks in SBF. The size of the spherulites is larger in the HCl-AH group, while the number of spherulites is higher in the Water-AH group. At 3–7 days, nearly the entire surface was covered with an apatite layer in all groups. The apatite-forming ability did not differ between the peripheral and central areas of the same implant.

3.2. *In vivo* evaluation

3.2.1. Gross inspection

All dogs tolerated the surgical procedure well. None exhibited infection of the surgical site, dislocation of the implants, or adverse reactions such as inflammation or foreign-body reactions on or around the implanted cylinders.

3.2.2. Histological findings

The HCl-AH group had superior osteoinductive ability compared with the other groups and exhibited induction of new bone within 3 months in all implants (Fig. 5). In the AH group at 3 months, no bone formation was detected in any implant (Fig. 5A), although granulation-like fibrous-connective tissue formation and newly formed blood vessels in the pore regions of the implant were observed (Fig. 5B). In the Water-AH group, a small amount of obvious bone formation with osteocytes was observed in one of four implants, but only a small amount of mineralized tissue suggesting osseous nidi was detected in the other three implants (Figs. 5C, D). At this time point in the HCl-AH group, optical microscopy showed a large amount of mineralized, newly formed bone containing osteocytes (Figs. 5E, F). Marrow-like tissue formation was also observed near the new bone (Fig. 5F). Around the new bone, osteoclast-like multinucleated cells and cuboidal osteoblast-like cells lining the new bone could be seen (Fig. 6A). Osteoclast-like multinucleated cells were also noted around the implant surface (Fig. 6B). No bone formation could be recognized at the outer surface of the porous blocks, and no crystal formations or pathological calcifications were observed. There was no sign of cartilage formation or endochondral ossification.

At 6 months postimplantation, three of four implants in the AH group and all implants in the Water-AH and HCl-AH groups had induced new bone. At 12 months, all implants in each group had induced new bone (Fig. 7A, B). In the HCl-AH group, an extensive amount of new bone developed in the pore regions of the implant. The new bone can be seen in the peripheral area of the implant as well as in the center area (Fig. 7B). In the AH group and Water-AH group, the new bone was limited in the center area (Fig. 7A), and the amount of new bone formation was less than that observed in the HCl-AH group. At this time, marrow-like tissue, cuboidal osteoblast-like cells, and

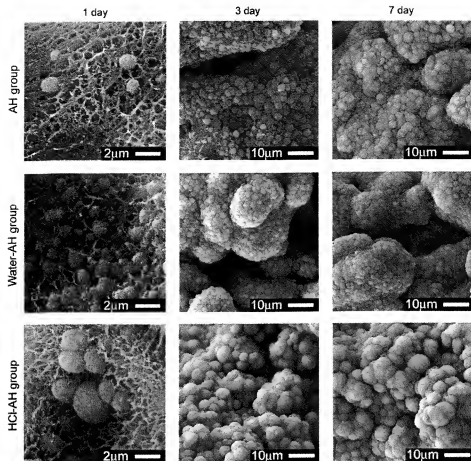


Fig. 4. SEM photographs of the surfaces of each implant after immersion in SBF for 1, 3 and 7 days. Note the larger size of the spherulites in the HCl-AH group, and the higher number of the spherulites in the Water-AH group. At 3–7 days, nearly the entire surface was covered with an apatite layer in all groups.

osteoclast-like multinucleated cells were still visible in the pores of each implant.

3.2.3. New bone area

The bone incidence (number of bone-induced samples/number of implanted samples) and new bone-area fraction (%) for each implant are shown in Fig. 8. At 3 months, the new bone fraction was $0.0\% \pm 0.0\%$ (bone incidence = 0/4) in the AH group, $0.5\% \pm 0.6\%$ (1/4) in the Water-AH group, and $8.3\% \pm 2.5\%$ (4/4) in the HCl-AH group. At 6 months, the new bone fraction was $2.2\% \pm 1.4\%$ (3/4) in the AH group, $4.8\% \pm 2.4\%$ (4/4) in the Water-AH group, and $11.6\% \pm 1.2\%$ (4/4) in the HCl-AH group. At 12 months, the respective values were $4.0\% \pm 5.8\%$ (3/3), $5.7\% \pm 3.2\%$ (3/3), and $20.3\% \pm 6.4\%$ (3/3). The new bone area was significantly larger in the HCl-AH group than in the other two groups at all postimplantation times ($P < 0.05$).

3.2.4. Surface observation of the inner pores after implantation

The inner pores of the porous titanium implants and newly induced bone were examined by observation of the

fractured surfaces of the implants (Figs. 9A–C). In the SEM examination of the HCl-AH implants at 3 months postimplantation, we observed a three-dimensional structure for the induced bone, which appeared to grow along the pore walls in all directions (Fig. 9A). Around the induced bone, apatite-like deposits containing Ca and P peaks in the SEM-EDX analysis could be recognized in some areas (Fig. 9B). In other areas apart from the induced bone, although obvious apatite-like deposits could not be observed, SEM-EDX analysis detected small Ca and P peaks on the surface of the treated layer (Fig. 9C). These small Ca and P peaks were also detected on the surface of the AH and Water-AH implants at 3 months when no obvious bone induction had occurred. We were unable to perform quantitative analysis of each implant using SEM-EDX because of the complex porous structures and very small Ca and P peaks.

4. Discussion

An irregular microporous titania layer was successfully formed on the surface of the porous titanium implants

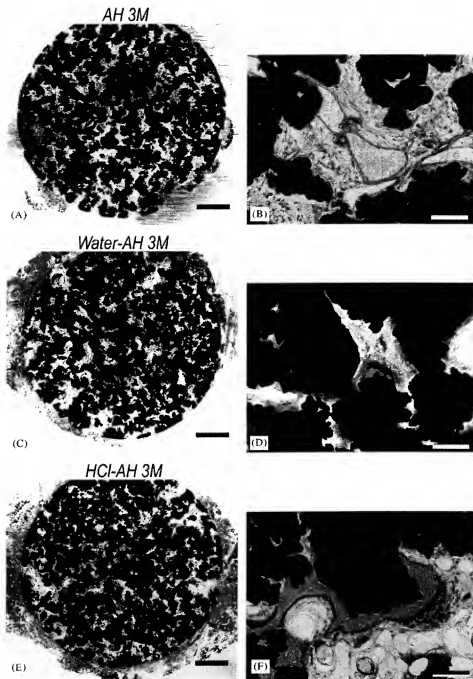


Fig. 5. Nondecalified histological sections of each implant after implantation in the muscles of beagle dogs for 3 months, shown at low magnification (A, C, E; bar = 1 mm) and high magnification (B, D, F; bar = 100 μ m). Stain: Stevenel's blue and Van Gieson's picrofuchsin. In the AH group (A, B), no bone formation but some vascular invasion can be seen. In the Water-AH group (C, D), a small amount of bone-like tissue indicating ossous nidi can be seen. In the HCl-AH group (E, F), obvious bone formation with osteocytes and marrow-like tissue can be seen.

following dilute HCl treatment coupled with conventional chemical and thermal treatments. The dilute HCl treatment was considered to have both chemical and topographic effects on the titanium surface. For the chemical effect, the dilute HCl treatment effectively removed sodium from the sodium titanate formed on the alkali-treated porous titanium and contributed to titania formation. For the

topographical effect, although not the initial purpose of the treatment, an etching effect was seen on the microporous surface. This HCl-AH treated porous bioactive titanium showed superior osteoinductive ability, and appeared to induce bone formation within 3 months. This induction period is much shorter than in a previous study of conventional Water-AH treated porous bioactive titanium

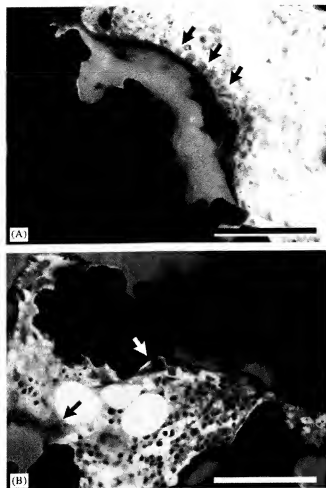


Fig. 6. Nondecalcified histological section of an HCl-AH implant after implantation in the muscles of beagle dogs for 3 months, shown at high magnification (bar = 100 μ m). Stain: Stevenel's blue and Van Gieson's picrofuchsin. (A) Cuboidal osteoblast-like cells (black arrow) can be seen. (B) Osteoclast-like multinucleated cells can be seen on both the bone (white arrow) and implant surface (black arrow).

implants in which bone induction was observed at 12 months [10].

Bone-like apatite layer formation on the pore surface in the early stages is believed to be the precursor to bone induction by non-CaP biomaterials and CaP-based porous ceramics [10–14]. This proposal was confirmed partially by SEM-EDX analysis, showing calcium and phosphate precipitation on the surface of the porous bioactive titanium. Previous studies of titanium plates have shown that the *in vitro* apatite-forming ability is higher in the titania layer than in the sodium titanate layer [18,21]. One possible explanation for the enhanced osteoinductivity of the HCl-AH implants is improved apatite-forming ability because of titania formation. However, we were unable to use SEM-EDX to analyze the *in vivo* apatite-forming ability of each implant quantitatively because of the complex porous structure and very small Ca and P peaks. Moreover, the *in vitro* apatite-forming abilities were too

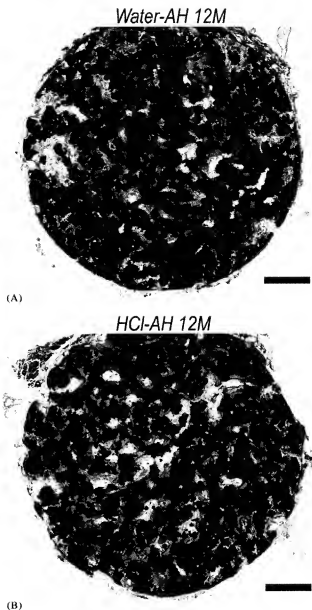


Fig. 7. Nondecalcified histological sections of a Water-AH implant (A) and a HCl-AH implant (B) after implantation in the muscles of beagle dogs for 12 months, shown at low magnification (bar = 1 mm). Stain: Stevenel's blue and Van Gieson's picrofuchsin. In the HCl-AH group, extensive new bone formation can be seen compared with the Water-AH group. The new bone area fraction was 9.4% in Fig. 7A (Water-AH implant) and 23.2% in Fig. 7B (HCl-AH implant). Note that in the HCl-AH implant, the new bone can be seen in the peripheral area of the implant as well as the center area, while in the Water-AH implant, it is limited in the center area.

high for comparison in all of the treated titanium groups, and apatite deposits were found only 1 day after soaking in SBF. The larger size of the apatite deposits in the HCl-AH group and the high number in the other groups also made quantitative *in vitro* analysis more complicated. At present, we cannot draw a conclusion about these differences in

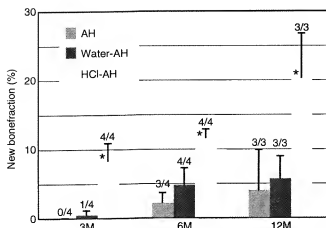


Fig. 8. Bone incidence and new bone-area fraction. The values above each bar represent the bone incidence (number of bone-induced samples/number of implanted samples). *: significant difference between the HCl-AH group and the other groups at each postimplantation time.

vitro behavior related to surface characteristic. It may be difficult to compare the in vivo performance of such highly bioactive implants with the in vitro apatite-forming ability alone, although the in vitro apatite-forming ability in SBF remains a very effective screening test for bioactivity [26].

The micropores on the macropore walls of the implants (topography) are considered another important factor in the osteoinductive ability of calcium phosphate ceramics [13,14]. The microporous surface of the HCl-AH implant was more complex than the other types of implants because it possessed a bimodal distribution of a combination of large and small micropores, giving a larger surface area. This specific microporous structure of the HCl-AH implants may have been caused by an etching effect of the dilute HCl treatment [28], although this effect was not the initial purpose of the treatment. This peculiar microporous structure may enhance protein adsorption and cell attachment, and may contribute to improved osteoinductivity.

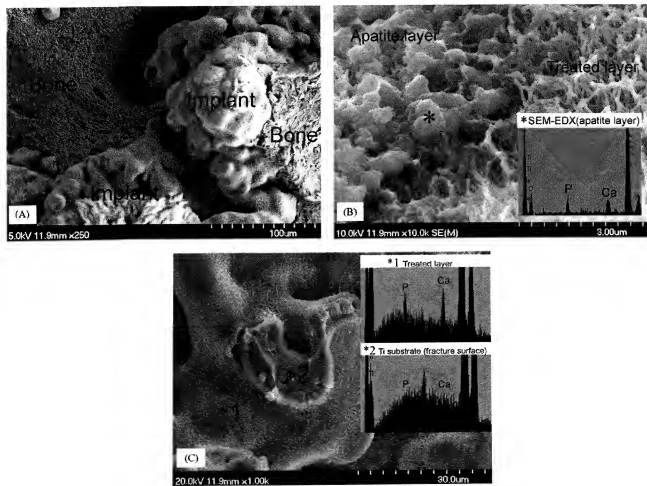


Fig. 9. SEM examination of the inner pores of the HCl-AH group after implantation in the muscles of beagle dogs for 3 months. (A) Observation of the inner surface and the induced bone. The image shows the three-dimensional structure of the induced bone growing along the implant surface in all directions. (B) Observation of the inner surface around the induced bone. *: apatite-like deposits containing Ca and P peaks in the SEM-EDX analysis can be seen. (C) Observation of the inner surface apart from the induced bone. *1: treated layer; *2: fracture surface of the titanium substrate. Small Ca and P peaks in the SEM-EDX analysis are apparent on the surface of the treated layer. Note that no Ca and P peaks are apparent on the fracture surface of the titanium substrate (negative control).

In addition to the possible explanations for the enhanced osteoinductivity of the HCl-AH porous titanium described above, many other physiological factors may contribute to the effects on osteoinductivity. For example, the sodium ion on the sodium titanate layer of the AH and the Water-AH implants seemed to have an adverse effect on the activity of osteogenic proteins or cells [29].

Both the surface chemistry and topography are important factors known to influence the biological response to biomaterials [30]. The results of the current study indicate that chemistry and topography are also linked with material-induced osteoinduction, although we cannot determine the predominant factor for the improved osteoinductivity following the dilute HCl treatment—surface chemistry (titanium formation and sodium removal) alternations or surface topography (etching) changes.

Even in an environment without mechanical stresses, bone induced by porous bioactive titanium does not disappear after 12 months. In a 2.5-year study in dogs, Yuan et al. [31] found normal compact bone with bone marrow in porous CaP ceramics. They considered the presence of bone marrow in the porous implant, which we also observed, as important for the long-term maintenance of bone after implantation; bone marrow might act as a supplier of mesenchymal cells [31]. In contrast, another study using CaP-coated porous metal implants detected no bone in the 24-week implants, even though the 12-week implants had demonstrated osteoinduction [9]. These authors suggested that bone induced by CaP coating degraded with time, and proposed that this degradation might be caused by interruption of the Ca^{2+} supply from the CaP coating. Our observation of increasing new bone area in our implants is an interesting phenomenon that indicates long-lasting bioactivity of the treated layer.

The mechanisms of osteoinduction by biomaterials and their biological effects are still largely unknown. A bone-like apatite layer on the surface of bioactive titanium can be a target for osteoclasts [27]. Osteoclast-like multinucleated cells observed on the pore surface may absorb this naturally occurring apatite layer, which may contribute to bone formation by osteoblasts in the remodeling process. Thus, osteoinductive porous implants covered by biological apatite may act like natural bone. We propose that osteoinductive porous biomaterials provide ideal conditions for bone growth in their pores.

Whether improvement of osteoinductivity would have a positive impact on orthotopic performance is controversial. Indeed, some of the critical factors for osteoinductivity may be unimportant for bone ingrowth in orthotopic sites. For example, as for macroporous structures, an interconnected concave pore structure is one of the prerequisites for an osteoinductive biomaterial to maintain the protected pore area without strong fluid movement [32]; in contrast, a convex pore structure, such as in a fiber mesh implant that is reported to have no osteoinductivity [10], is not a drawback in orthotopic sites where bone ingrowth from the periphery can be expected [33]. Conversely, the surface

characteristics for the improved osteoinductivity observed in this study—titanium formation and complex topography—appear to parallel those required for higher osteoinductivity [21,28,30]. Furthermore, in unfavorable conditions where sufficient bone ingrowth from the periphery cannot be expected, such as with the existence of a gap [9] or in large bone defect [34], osteoinductive properties are theoretically attractive even in orthotopic use. Therefore, we consider that in developing porous biomaterials, ectopic performance should be controlled, to say nothing of the orthotopic performance. With this point of view, adding a dilute HCl treatment to the conventional chemical and thermal treatment is a promising candidate for advanced surface treatment of porous titanium implants.

5. Conclusion

Dilute HCl treatment effectively removed sodium from the sodium titanate layer of alkali-treated porous titanium and contributed to the formation of the titanium layer on the surface of porous bioactive titanium. Furthermore, the HCl-AH implants possessed a more complex surface than other implants, which may have been caused by an etching effect of the dilute HCl treatment. The HCl-AH implants exhibited better osteoinductivity and induced ectopic bone growth in the back muscles of beagle dogs within 3 months. The results of this study indicate that chemistry and topography are also related to material-induced osteoinduction, although we cannot determine the predominant factor for the improved osteoinductivity following the dilute HCl treatment—surface chemistry (titanium formation and sodium removal) or surface topography (etching) changes.

Acknowledgments

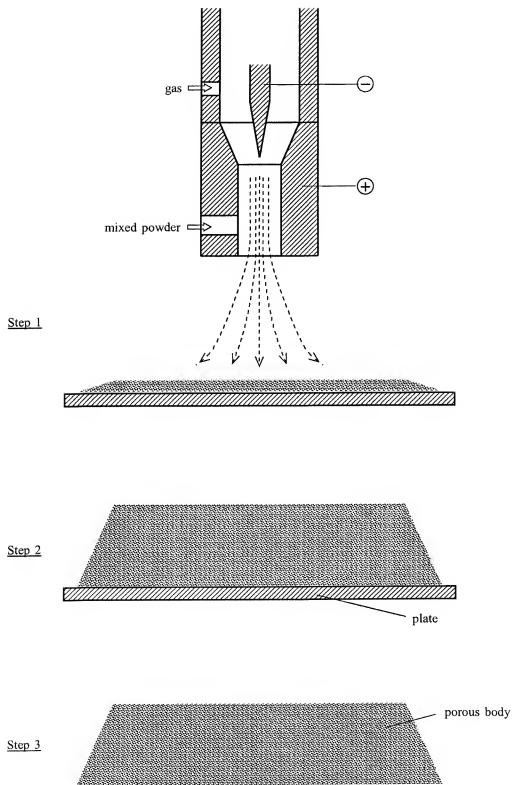
This research was partially supported by the Japanese Ministry of Education, Science, Sports and Culture through a Grant-in-Aid for Scientific Research (A) number 16200035.

References

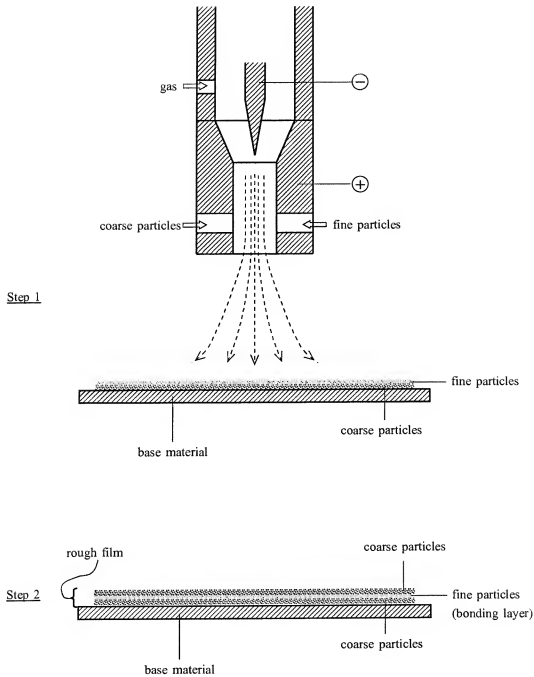
- [1] Hench LL, Wilson J. Introduction to bioceramics. Singapore: World Scientific; 1993.
- [2] Yang Z, Yuan H, Tong W, Zou P, Chen W, Zhang X. Osteogenesis in extraskeletally implanted porous calcium phosphate ceramics: variability among different kinds of animals. *Biomaterials* 1996;17: 2131–7.
- [3] Yuan HP, De Bruijn JD, Li YB, Feng JQ, Yang ZJ, De Groot K, et al. Bone formation induced by calcium phosphate ceramics in soft tissue of dogs: a comparative study between porous alpha-TCP and beta-TCP. *J Mater Sci Mater Med* 2001;12:7–13.
- [4] Yuan H, De Bruijn JD, Zhang X, van Blitterswijk CA, de Groot K. Bone induction by porous glass ceramic made from Bioglass (45S5). *J Biomed Mater Res* 2001;58:270–6.
- [5] Yamasaki H, Sakai H. Osteogenic response to porous hydroxyapatite ceramics under the skin of dogs. *Biomaterials* 1992;13:308–12.

- [6] Ripamonti U. The morphogenesis of bone in replicas of porous hydroxyapatite obtained from conversion of calcium carbonate exoskeletons of coral. *J Bone Joint Surg Am* 1991;73:692–703.
- [7] Yuan HP, Yang ZJ, Li YB, Zhang XD, De Bruijn JD, De Groot K. Osteoinduction by calcium phosphate biomaterials. *J Mater Sci Mater Med* 1998;9:723–6.
- [8] Habibovic P, Li J, Van der Valk CM, Meijer G, Layrolle P, Van Blitterswijk CA, et al. Biological performance of uncoated and octacalcium phosphate-coated Ti6Al4V. *Biomaterials* 2005;26:23–36.
- [9] Barrere F, van der Valk CM, Dalmeyer RA, Meijer G, van Blitterswijk CA, de Groot K, et al. Osteogenicity of octacalcium phosphate coatings applied on porous metal implants. *J Biomed Mater Res* 2003;66A:779–88.
- [10] Fujibayashi S, Neo M, Kim HM, Kokubo T, Nakamura T. Osteoinduction of porous bioactive titanium metal. *Biomaterials* 2004;25:443–50.
- [11] Winter GD, Simpson BJ. Heterotopic bone formation in a synthetic sponge in the skin of young pigs. *Nature* 1969;223:88–90.
- [12] Yang ZJ, Yuan HP, Zou P, Tong WD, Qu SX, Zhang XD. Osteogenic responses to extracranially implanted synthetic porous calcium phosphate ceramics: an early stage histomorphological study in dogs. *J Mater Sci Mater Med* 1997;8:697–701.
- [13] Habibovic P, Yuan H, van der Valk CM, Meijer G, van Blitterswijk CA, de Groot K. 3D microenvironment as essential element for osteoinduction by biomaterials. *Biomaterials* 2005;26:3565–75.
- [14] Yuan HP, Kurashina K, de Bruijn JD, Li YB, de Groot K, Zhang XD. A preliminary study on osteoinduction of two kinds of calcium phosphate ceramics. *Biomaterials* 1999;20:1799–806.
- [15] Kokubo T, Miyaji F, Kim HM, Nakamura T. Spontaneous formation of bonelike apatite layer on chemically treated titanium metals. *J Am Ceram Soc* 1996;79:1127–9.
- [16] Kim HM, Miyaji F, Kokubo T, Nishiguchi S, Nakamura T. Graded surface structure of bioactive titanium prepared by chemical treatment. *J Biomed Mater Res* 1999;45:100–7.
- [17] Nishio K, Neo M, Akiyama H, Nishiguchi S, Kim HM, Kokubo T, et al. The effect of alkali- and heat-treated titanium and apatite-formed titanium on osteoblastic differentiation of bone marrow cells. *J Biomed Mater Res* 2000;52:652–61.
- [18] Uchida M, Kim HM, Kokubo T, Fujibayashi S, Nakamura T. Effect of water treatment on the apatite-forming ability of NaOH-treated titanium metal. *J Biomed Mater Res* 2002;63:522–30.
- [19] Nishiguchi S, Fujibayashi S, Kim HM, Kokubo T, Nakamura T. Biology of alkali- and heat-treated titanium implants. *J Biomed Mater Res* 2003;67A:26–35.
- [20] Nishiguchi S, Kato H, Fujita H, Oka M, Kim HM, Kokubo T, et al. Titanium metals form direct bonding to bone after alkali and heat treatments. *Biomaterials* 2001;22:2525–33.
- [21] Fujibayashi S, Nakamura T, Nishiguchi S, Tamura J, Uchida M, Kim HM, et al. Bioactive titanium: effect of sodium removal on the bone-bonding ability of bioactive titanium prepared by alkali and heat treatment. *J Biomed Mater Res* 2001;56:562–70.
- [22] Nishiguchi S, Nakamura T, Kobayashi M, Kim HM, Miyaji F, Kokubo T. The effect of heat treatment on bone-bonding ability of alkali-treated titanium. *Biomaterials* 1999;20:491–500.
- [23] Takemoto M, Fujibayashi S, Neo M, Suzuki J, Kokubo T, Nakamura T. Mechanical properties and osteoconductivity of porous bioactive titanium. *Biomaterials* 2005;26:6014–23.
- [24] Abe Y, Kokubo T, Yamamuro T. Apatite coating on ceramics, metals and polymers utilizing a biological process. *J Mater Sci Mater Med* 1990;1:239–44.
- [25] Kokubo T, Kushitani H, Sakka S, Kitsugi T, Yamamuro T. Solutions able to reproduce in vivo surface-structure changes in bioactive glass-ceramic A-W. *J Biomed Mater Res* 1990;24:721–34.
- [26] Fujibayashi S, Neo M, Kim HM, Kokubo T, Nakamura T. A comparative study between in vivo bone ingrowth and in vitro apatite formation on Na₂O–CaO–SiO₂ glasses. *Biomaterials* 2003;24:1349–56.
- [27] Matsuoka H, Nakamura T, Takadama H, Yamada S, Tamura J, Okada Y, et al. Osteoclastic resorption of bone-like apatite formed on a plastic disk as an in vitro assay system. *J Biomed Mater Res* 1998;42:278–85.
- [28] Hacking SA, Harvey EJ, Tanzer M, Krygier JJ, Bobyn JD. Acid-etched microtexture for enhancement of bone growth into porous-coated implants. *J Bone Joint Surg Br* 2003;85:1182–9.
- [29] Chou L, Marek B, Wagner WR. Effects of hydroxylapatite coating crystallinity on biocompatibility, cell attachment efficiency and proliferation in vitro. *Biomaterials* 1999;20:977–85.
- [30] Hacking SA, Tanzer M, Harvey EJ, Krygier JJ, Bobyn JD. Relative contributions of chemistry and topography to the osseointegration of hydroxyapatite coatings. *Clin Orthop Relat Res* 2002;24–38.
- [31] Yuan HP, Yang ZJ, de Bruijn JD, de Groot K, Zhang XD. Material-dependent bone induction by calcium phosphate ceramics: a 2.5-year study in dog. *Biomaterials* 2001;22:2617–23.
- [32] Habibovic P, Van der Valk CM, Van Blitterswijk CA, De Groot K, Meijer G. Influence of octacalcium phosphate coating on osteoinductive properties of biomaterials. *J Mater Sci Mater Med* 2004;15:373–80.
- [33] Chang Y-S, Gu H-O, Kobayashi M, Oka M. Influence of various structure treatments on histological fixation of titanium implants. *J Arthroplasty* 1998;13:816–25.
- [34] Habibovic P, van den Doel M, van Blitterswijk CA, De Groot K. Performance of osteoinductive biphasic calcium-phosphate ceramic in a critical-sized defect in goats. *Koy Eng Mater* 2006;309–311:1303–6.

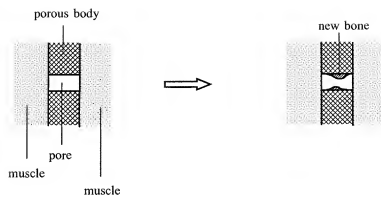
Referential Fig.1



Referential Fig.3



Referential Fig.2



Referential Fig.4

